

**Nina Tiralla^{1*}, Oleg Panferov², Heinrich Kreilein¹, Alexander Olchev^{3,4},
Ashehad A. Ali¹ and Alexander Knohl¹**

¹ University of Goettingen, Bioclimatology, Göttingen, Germany

² University of Applied Sciences Bingen, Dept. of Life Sciences and Engineering, Bingen, Germany

³ Moscow State University, Faculty of Geography, Moscow, Russia

⁴ Severtsov Institute of Ecology and Evolution, Russian Academy of Sciences, Moscow, Russia

* **Corresponding author:** ntirall1@gwdg.de

QUANTIFICATION OF LEAF EMISSIVITIES OF FOREST SPECIES: EFFECTS ON MODELLED ENERGY AND MATTER FLUXES IN FOREST ECOSYSTEMS

ABSTRACT. Climate change has distinct regional and local differences in its impacts on the land surface. One of the important parameters determining the climate change signal is the emissivity (ϵ) of the surface. In forest-climate interactions, the leaf surface emissivity plays a decisive role. The accurate determination of leaf emissivities is crucial for the appropriate interpretation of measured energy and matter fluxes between the forest and the atmosphere. In this study, we quantified the emissivity of the five broadleaf tree species *Acer pseudoplatanus*, *Fagus sylvatica*, *Fraxinus excelsior*, *Populus simonii* and *Populus candicans*. Measurements of leaf surface temperatures were conducted under laboratory conditions in a controlled-climate chamber within the temperature range of +8 °C and +32 °C. Based on these measurements, broadband leaf emissivities ϵ (ϵ for the spectral range of 8-14 μm) were calculated. Average $\epsilon_{8-14\mu\text{m}}$ was 0.958 ± 0.002 for all species with very little variation among species. In a second step, the soil-vegetation-atmosphere transfer model 'MixFor-SVAT' was applied to examine the effects of ϵ changes on radiative, sensible and latent energy fluxes of the Hainich forest in Central Germany. Model experiments were driven by meteorological data measured at the Hainich site. The simulations were forced with the calculated ϵ value as well as with minimum and maximum values obtained from the literature. Significant effects of ϵ changes were detected. The strongest effect was identified for the sensible heat flux with a sensitivity of 20.7 % per 1 % ϵ change. Thus, the variability of ϵ should be considered in climate change studies.

KEY WORDS: Leaf emissivity, matter flux, energy flux, MixFor-SVAT

CITATION: Nina Tiralla, Oleg Panferov, Heinrich Kreilein, Alexander Olchev, Ashehad A. Ali, Alexander Knohl (2019) Quantification of leaf emissivities of forest species: Effects on modelled energy and matter fluxes in forest ecosystems. *Geography, Environment, Sustainability*,

Vol.12, No 2, p. 245-258

DOI-10.24057/2071-9388-2018-86

INTRODUCTION

Impacts of climate change on regional as well as on local scales differ spatially substantially. Some of the reasons for this spatial variability is local and regional as land use and land cover differences as well land use changes, which bring along variations in surface properties (Pielke et al. 2011). The impact of forest specific land use changes such as anthropogenic deforestation and the effect of forest biomes in general on climate is extensively discussed in the scientific literature (Alkama and Cecatti 2016; Snyder et al. 2004 among many others). The strength of the forest-climate interactions and the magnitude of the contribution of the forest to climate variability and to climate change depends strongly on forest properties such as canopy structure, albedo, and surface roughness (Bonan 2008). One of the important forest parameters is the surface emission coefficient or emissivity (ϵ), which determines the radiation emission via the Stefan-Boltzmann law, and thus directly affects net radiation. That in turn regulates the radiative cooling and warming of the surface, and thus determines surface temperatures, which affect the local and regional climate (Sabajo et al. 2017). Information on surface emissivity is crucial for an accurate interpretation of measured energy and matter fluxes between forest and the atmosphere, for the interpretation of remote sensing data and for an appropriate parameterization of biomes in land surface models (Jin and Liang 2006).

For almost two decades, several studies have focused on estimating specified emissivity values for different land covers and plant functional types (da Luz and Crowley 2007; Jin and Liang 2006; Valor and Caselles 1996). However, there is no consensus on how to measure emissivity accurately because emissivity of forested surfaces may vary with surface properties such as tree species composition, plant growth stage, surface roughness, leaf area index and water content (Zhou et al. 2008). Aside from that, the emissivity of a forest canopy as a whole differs from that of individual leaves. This is also true for monocultures, since the

canopy emissivity is defined by a composition of different surfaces such as the ones of leaves, stems, understory plants and soil and it is also affected by the “cavity effect” (Jin and Liang 2006; Fuchs and Tanner 1966). For the direct estimation of broadband emissivity in the 8-13 μm wavelength band ($\epsilon_{8-13\mu\text{m}}$) of individual leaves, Fuchs and Tanner (1966) used infrared (IR)-thermometer and 0.08 mm iron-constantan thermocouples inserted into leaves of tobacco and snap bean to measure their leaf surface temperature. They obtained $\epsilon_{8-13\mu\text{m}}$ values of 0.971 ± 0.002 and 0.957 ± 0.005 , respectively. For dense canopies of tall sudangrass and alfalfa, Fuchs and Tanner (1966) identified canopy emissivities of 0.976 and 0.977, respectively. A similar, but more advanced approach in terms of reproducibility, was made by Idso et al. (1969), who found $\epsilon_{8-13\mu\text{m}}$ values between 0.969 and 0.977 for different forest species (Table 1). Leaf emissivity values measured in forests and horticulture (Chen 2015; Lopez et al. 2012; Rahkonen and Jokela 2003; Arp and Phinney 1980) are summarized in Table A.1 of the Appendix.

The estimation of ϵ by remote sensing is more complicated, since it additionally requires information on the surface temperature at the particular moment of the satellite or airborne measurement. Considering this, the remote sensing study by Valor and Caselles (1996) used indirect estimations of emissivity. They estimated the emissivity of the spectral region between 10.5 to 12.5 μm using satellite measurements of infrared radiation and normalized difference vegetation index (NDVI). Da Luz and Crowley (2007) estimated spectral emissivity of forest leaves, ϵ_{λ} , with spectral measurements. However, their approach was ground based - under laboratory conditions and in the field. In their study, surface temperature was approximated indirectly through an iterative method also used in Horton et al. (1998). Da Luz and Crowley (2007) showed that the ϵ_{λ} of forest tree species varies considerably in the spectral region of 8 to 13 μm : for American beech (*Fagus grandifolia*) from 0.94 to 0.97 and for red maple (*Acer rubrum*) from 0.942 to 0.973. To evaluate

Table 1. Leaf emissivities ($\epsilon \pm \text{s.d.}$) of different forest species

Species	ϵ	References
<i>Acer rubrum</i>	0.942 - 0.973	Da Luz & Crowley (2007)
<i>Catalpa speciosa</i>	0.938 - 0.973	Da Luz & Crowley (2007)
<i>Cornus florida</i>	0.962 - 0.985	Da Luz & Crowley (2007)
<i>Fagus grandifolia</i>	0.940 - 0.970	Da Luz & Crowley (2007)
<i>Hedera helix var. Algerian</i>	0.969 \pm 0.005	Idso et al. (1969)
<i>Ligustrum vulgare cv. Japanese</i>	0.964 \pm 0.003	Idso et al. (1969)
<i>Liriodendron tulipifera</i>	0.948 - 0.973	Da Luz & Crowley (2007)
<i>Morus alba</i>	0.976 \pm 0.008	Idso et al. (1969)
<i>Populus fremontii</i>	0.977 \pm 0.004	Idso et al. (1969)
<i>Prunus serotina</i>	0.945 - 0.967	Da Luz & Crowley (2007)

the effects of ϵ variability on climate modelling results, Jin and Liang (2006) converted the spectral emissivities, ϵ_{λ} , obtained from the remote sensing platform MODIS into the broadband emissivity, $\epsilon_{8-13\mu\text{m}}$. They investigated the effect of measured vs. fixed emissivity values onto the climate by using the Community Land Model, CLM2. The main focus of those sensitivity studies was the comparison of radiation, sensible and latent energy fluxes under following assumptions: 1) the default ϵ value of 0.96 for bare soil and 0.97 for vegetation and 2) under an estimated value of 0.9 for bare soil, keeping 0.97 for vegetation-covered regions. The results of the global simulations show surface temperature changes of ± 1 °C (January 1998) for the offline CLM simulation and up to 1.5 °C temperature decrease for the coupled CAM2-CLM2 simulation. Furthermore, changes of the sensible heat flux (new value minus control run) were -1 Wm^{-2} to $+5 \text{ Wm}^{-2}$. Due to the fact that the highest sensitivity to ϵ values was identified for desert areas, a separate run was performed for Tucson, Arizona, for the year 1993. The results showed changes of daily surface temperatures up to 10 °C and changes of diurnal sensible and latent heat fluxes up to 50 Wm^{-2} , whereas the changes in sensible heat were always positive (Jin and Liang 2006).

These findings show that the poorly constrained value of emissivity substantially contributes to uncertainties in land surface models and thus to a quantification of climate change signals. Consequently, it is necessary to estimate the emissivity as accurate as possible and to cover many different land surfaces and plant species.

Thus, our goals are (1) to measure the broadband emissivities $\epsilon_{8-14, \mu\text{m}}$ of five different broadleaf tree species by using a direct approach similar to that of Fuchs and Tanner (1966), i.e. applying infrared-pyrometer and thermocouples onto leaf surfaces, and (2) to integrate the measured emissivity into a modeling framework (MixFor-SVAT) and investigate the sensitivity of modeled variables (outgoing longwave radiation, net radiative balance, latent and sensible heat fluxes, canopy temperature and net ecosystem exchange) to changes in emissivity.

MATERIAL AND METHODS

Study site

The Hainich tower site in Central Germany serves as reference site for this study. It is located within the southern part of the 'Hainich National Park' (51°04'46"N, 10°27'08"E, 440 m a.s.l.) in suboceanic/subcontinental climate (Knobl et al. 2003). At the Hainich flux tower,

measurements of carbon dioxide, water vapor and energy fluxes between the forest and the atmosphere as well as microclimate in the forest are made. The flux tower is placed in an old unmanaged mixed beech forest with a highly heterogeneous age class distribution ranging from 0 to 250 years and a maximum height varying between 30 and 35 m. The forest is dominated by European beech (*Fagus sylvatica*) with 65 %, codominated by the secondary tree species European ash (*Fraxinus excelsius*) with 25 %, followed by maple (*Acer pseudoplatanus* and *A. platanoides*) with 7 %. Several other deciduous and coniferous species are interspersed (Anthoni et al. 2004). The maximum leaf area index is $5.0 \text{ m}^2 \text{ m}^{-2}$ (Knobl et al. 2003). The Hainich tower site (DE-Hai) is apart of the European Integrated Carbon Observation network (ICOS, <https://www.icos-ri.eu/>) and the global eddy covariance station network FLUXNET (<http://fluxnet.fluxdata.org/>).

Instrumentation

For the direct estimations of $\epsilon_{8-14\mu\text{m}}$ of the chosen tree species, we applied a direct method similar to that of Fuchs and Tanner (1966). The surface temperature of leaves was measured simultaneously by means of digital infrared pyrometers (IN510-N, Omega Engineering Inc., Deckenpfronn, Germany) and thermocouples inserted under the skin of the leaves. The IN510-N had a default emission factor of $\epsilon_{\text{IR}} = 0.95$, a 2:1 field of view and a spectral range of $8 \mu\text{m}$ to $14 \mu\text{m}$. We used two types of thermocouples; type K (NiCr-Ni, DIN class 1, \varnothing : 0.08 mm, TC Direct, Mönchengladbach, Germany) and type T (Cu-CuNi, \varnothing : 0.2 mm, TC Direct, Mönchengladbach, Germany). Temperatures were continuously logged using two eight-channel RedLab USB TC measuring units (Meilhaus Electronic GmbH, Alling, Germany). For the calibration of the thermocouples, a reference thermometer (Hg thermometer, 0.01 °C resolution, Karl Schneider & Sohn oHG, Wertheim, Germany) was used. The ambient conditions, air temperature and air humidity, were measured by a thermo-hygrometer (Hygroclip with ROTRONIC HYGROMER® IN-1 and PT100 1/3 DIN Klasse B, Rotronic, Ettlingen, Germany) with an accuracy of $\pm 0.8 \%$ rh and $\pm 0.2 \text{ K}$. For data recording, a data logger (CR 1000, Campbell Scientific

Ltd., Logan, UT, USA) was used. Thermocouple measurements were performed every second and averaged over the period of one minute, whereas pyrometer measurements happened at a minutely base. The readings of the reference thermometer were done manually with a frequency of 20 minutes.

Calibrations

Thermocouples: We carried out calibration of the thermocouples in distilled water by means of a close-system water bath. The insulated container was surrounded by a heating film and contained a magnetic stirrer. The thermocouples were calibrated against a reference mercury thermometer within the range of +7 °C and +43 °C. To perform the calibration at low temperatures, several ice cubes were put into the water. Then the water with ice warmed up at room temperature. For temperatures higher than room's temperature, we heated up the water by means of the heating film. After that it continuously cooled down itself at room temperature. We repeatedly performed these calibration runs. Based on the calibration data, we calculated a linear calibration function for each sensor respectively. After the calibration, the thermocouples do not differ significantly under $\alpha=0.05$.

Digital infrared-pyrometer: To obtain the absolute calibration, we took one random pyrometer to calibrate it against the calibration source IRS-350 (Voltcraft®, Conrad Electronics, Wernberg-Köblitz, Germany). This reference pyrometer was then used for the cross-calibration of the other four pyrometers deployed during the experiment. We carried out the cross-calibration in a climate chamber by using an open-system water bath filled with distilled water ($\epsilon = 0.96$ at 20 °C according to Wolfe and Zissis 1978). The chamber was repeatedly heated up and cooled down within the range of +8 °C to +30 °C. Using these results, we calculated a linear calibration function for each sensor, which resulted in an absolute error range of $\pm 0.4 \text{ °C}$.

Measurements

For the quantification of the species specific leaf emissivities, we chose *Populus simonii*

and *Populus candicans* additionally to the dominant tree species of the Hainich site for the experimental setup.

The experimental study was carried out under stable climatic conditions in a climate chamber with temperature thresholds of +8 °C and +32 °C reflecting the range of temperatures at the Hainich site during the growing season. The experiments were performed for each of the chosen tree species separately. We put a minimum of 3 young trees of one species into the chamber. The surface temperature of a leaf was measured with a digital infrared pyrometer and two thermocouples: type K and type T. In case of the populous species, we also measured both, the adaxial and abaxial sides, of the leaves. The pyrometers were placed vertically in a distance of 4 cm above the leaf, whereas both thermocouples were directly affixed on the leaf surface right next to each other. Ambient air temperature and air humidity were recorded. We performed the experiments at absolute darkness, in order to avoid disturbance by short-wave radiation, for several days in a row; meanwhile the chamber temperature was continuously heated up and down within the range of 10 °C to 30 °C. The heating process was carried out in 5° C steps (5 hours) with 7 hours stabilising breaks in between. The broadband emissivities, $\epsilon_{8-14\mu\text{m}}$ of each leaf (from hereon called emissivity) were then calculated from the comparison of directly measured and radiative leaf temperatures based on the Stefan-Boltzmann law (eq. (1)).

$$\epsilon_{\text{leaf}} = \frac{T_{\text{sur}}^4_{\text{IR}} \times \epsilon_{\text{IR}}}{T_{\text{sur}}^4_{\text{Tc}}}$$

where:

$T_{\text{sur}}_{\text{IR}}$ is surface temperature measured with IR-pyrometer (8-14 μm spectral range),

$T_{\text{sur}}_{\text{Tc}}$ is surface temperature measured with thermocouples,

ϵ_{IR} is default emission factor (s. Material and Methods).

Modelling

We applied the model MixFor-SVAT to determine the effect of emissivity variations on mass and energy exchange at a local scale. The model experiments with MixFor-SVAT

were performed with the static broadband emissivity obtained in our present study ($\epsilon_{8-14\mu\text{m}} = 0.958$) as well as with the minima ($\epsilon = 0.94$) and maxima ($\epsilon = 0.97$) leaf emissivity for forest tree species found in scientific literature (da Luz and Crowley 2007). The model simulations were driven by meteorological data (air temperature, water vapor pressure, wind speed, precipitation rate, and global radiation) of the Hainich tower site for the years 2008 and 2009. MixFor-SVAT calculates the energy and matter fluxes between the atmosphere and the forest, including downward longwave radiation. As indicator parameters, outgoing longwave radiation (LRup [Wm^{-2}]), net radiative balance (Rn [Wm^{-2}]), latent (LE [Wm^{-2}]) and sensible (H [Wm^{-2}]) heat fluxes, canopy temperature (Tc [°C]), net ecosystem exchange (NEE [$\mu\text{molCO}_2\text{m}^{-2}\text{s}^{-1}$]) and the physical storage term of soil heat flux and canopy storage (PS [Wm^{-2}]) were selected.

MixFor-SVAT is a one-dimensional process based soil-vegetation-atmosphere transfer (SVAT) model, enabling the description of radiation transfer, plant transpiration and water uptake, as well as the turbulent exchange of carbon dioxide, sensible and latent heat between mono- and multi-species forest stands and the atmospheric surface layer (Olchev et al. 2008; Falge et al. 2005; Olchev et al. 2002). The plant canopy is assumed to be horizontally uniform and vertically structured. For the simulation of exchange processes, MixFor-SVAT uses a detailed description of biophysical properties of the different tree species such as the mean tree height, crown shape, leaf area density distribution, tree diameter at breast height, leaf stomatal conductance, parameters describing the photosynthesis and respiration including the kinetic properties of Rubisco, the dependence of electron transport on incoming photosynthetically active radiation, rate of dark respiration and others. The model is modularized and describes the following processes: radiative transfer (shortwave and longwave radiation), turbulent exchange of momentum, sensible heat, H₂O and CO₂ within and above a forest canopy, soil heat and water dynamics, plant water use, precipitation interception and net- and gross ecosystem production. The simulation procedure of the radiative transfer in a plant canopy takes into account

the different optical and structural properties of various tree species as well as annual leaf area index changes regulated by tree phenology (e.g. date of emergence of leaves, the onset of leaf fall, etc.). The broadband emissivity in the model is assumed to be constant for all vegetation types ($\epsilon = 0.96$). The longwave radiation absorption is calculated according to Kirchhoff's law ($\alpha = \epsilon$). The calculation of the radiation energy, water and CO₂ fluxes for Hainich forest were provided with a time step of 30 minutes. Maximum tree height in the forest canopy was assumed to be 31 m and the maximum LAI of the forest canopy as 6.06 m² m⁻². Gaps in the NEE, LE and H measurement records were filled using an approach based on a process-based MixFor-SVAT model (Olchev et al. 2015). MixFor-SVAT well simulated the observed surface fluxes, e.g. net radiation ($R^2 = 0.96$, slope = 0.996, $p < 0.001$).

RESULTS

Quantification of leaf emissivities for different tree species

Direct leaf surface temperature measurements using the T and K type thermocouples showed very good agreement with a temperature difference of less than 0.001 °C indicating no systematic differences between both thermocouples types. Leaf temperature measured with the infrared pyrometer was strongly linearly correlated to the direct measurements using thermocouples ($p < 0.001$ for all sensors). The measured broadband ϵ of the five investigated species varied only slightly (Table 2, Table A.1). The highest leaf emissiv-

ity is 0.960 ± 0.003 for *Fagus sylvatica* and the lowest 0.954 ± 0.003 for *Populus simonii*. The mean calculated emissivity of all species is 0.958 with a standard deviation of 0.002. According to Dunn's Multiple Comparison Test, there are only significant differences between the emissivities of *Populus simonii* ($\epsilon = 0.954$) and the non-populous species. No temperature dependencies of the leaf emissivity could be detected within the investigated range of +8 to +32 °C: $\epsilon_{8-14\mu m}$ varied by ± 0.0026 .

Effects of a change in emissivity on the energy and matter fluxes at a local scale

Three MixFor-SVAT simulations with a static broadband ϵ of 0.94, 0.958 (our mean value) and 0.97, respectively, were performed for the Hainich tower site for the period of 2008 and 2009. As seen in figure 1, mean annual values of LRup increase with an increase in broadband emissivity, whereas the mean annual values of Rn, Tc, LE, H and NEE decrease. The same trend can be observed for both years. However, the results indicate that the responses of the fluxes are non-linear.

While the differences between the respective values of both years seem to be similar for most parameters, the decrease of LE and Rn in 2009 is slightly stronger than in 2008. One possible reason for this is the higher amount of incoming shortwave radiation in 2008 which compensates the longwave emission losses - the shortwave radiation balance in 2008 was in average 8 Wm⁻² higher than in 2009.

The comparison of modelled and measured

Table 2. Leaf emissivity (ϵ) of five different broadleaf species

Tree species	ϵ
<i>Acer pseudoplatanus</i>	0.959 ± 0.003 a
<i>Fagus sylvatica</i>	0.960 ± 0.003 a
<i>Fraxinus excelsior</i>	0.958 ± 0.002 a
<i>Populus candicans</i>	0.957 ± 0.003 ab
<i>Populus simonii</i>	0.954 ± 0.003 b
total	0.958 ± 0.002

*Emissivities are displayed as mean \pm s.d.. Groups sharing the same letter are not significantly different ($p < 0.05$, Dunn's Multiple Comparison Test).

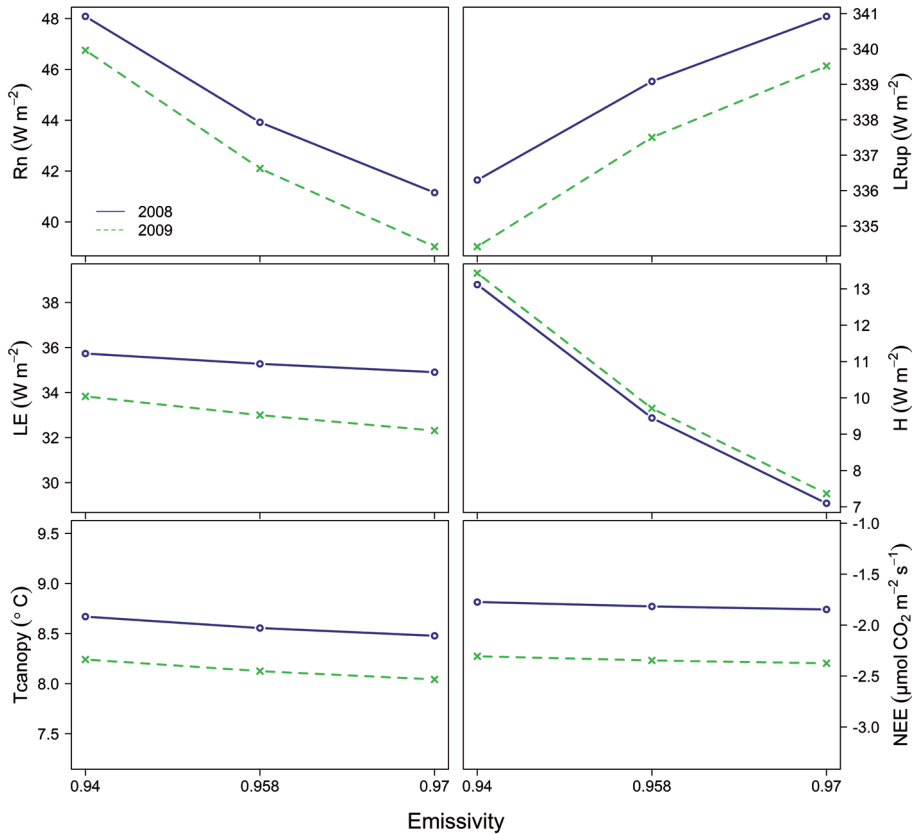


Fig.1. Dependency of energy and matter fluxes on changes in broadband emissivity. Mean annual values of the net radiative balance (Rn), outgoing longwave radiation (LRup), canopy temperature (Tcanopy), latent heat (LE), sensible heat (H) fluxes and net ecosystem exchange (NEE) calculated according to MixFor-SVAT model runs with $\epsilon = 0.94$, $\epsilon = 0.958$ (our mean value) and $\epsilon = 0.97$ for the years 2008 and 2009

data (Table 3) shows that in the case of LRup, Rn and NEE, measured data are higher than the modelled ones for 2008 and 2009. In 2008, measured H data are higher than modelled ones, whereas they are similar for 2009. On the contrary, for LE the measured data for

2008 are below the modelled data and for 2009 they are similar. The measured and the modelled canopy temperatures agree well for both years.

The relative changes of fluxes are shown

Table 3. Comparison of measured and MixFor-SVAT-modelled energy and matter fluxes

	year	Rn [Wm ⁻²]	LE [Wm ⁻²]	H [Wm ⁻²]	NEE [μmol CO ₂ m ⁻² s ⁻¹]	LRup [Wm ⁻²]	Tc [°C]
MixFor-SVAT	2008	48.09 - 41.15	35.75 - 34.1	13.12 - 7.1	-1.77 - -1.85	336.3 - 340.92	8.7 - 8.48
measured	2008	60.35	31.6	20.47	-1.66	355.92	8.65
MixFor-SVAT	2009	46.75 - 39.03	33.83 - 32.31	13.44 - 7.36	-2.31 - -2.37	334.42 - 339.52	8.2 - 8.04
measured	2009	60.85	33.79	13.18	-1.95	355.58	8.31

*MixFor-SVAT-modelled data are given as ranges due to simulations with emissivities of $\epsilon=0.94$, $\epsilon=0.958$ and $\epsilon=0.97$

in Fig. 2. The flux values obtained with the mean emissivity measured in the present study (0.958) are taken as reference. The relative changes are calculated as $\Delta Flux = \frac{(Flux - Flux_{Ref})}{Flux_{Ref}} \times 100\%$ (2). The relative changes were estimated for

$$\Delta Flux = \frac{(Flux - Flux_{Ref})}{Flux_{Ref}} \times 100\% \quad (2)$$

above calculated indicators and additionally for PS.

For 2008, the largest relative difference is found for the sensible heat flux. A decrease of 0.018 in emissivity ($\epsilon = 0.94$) results in an increase of H, indicating a sensitivity of 20.7 % per 1 % of ϵ change. The change from 0.958 to 0.97 (0.012) causes a decrease of H, denoting a relative sensitivity of -19.9 % per 1 % of ϵ change. All other fluxes show less sensitivity to ϵ . For Rn, a decrease of 0.018 in emissivity produces

an expected increase of radiative balance, implying a relative sensitivity of 5.0 % per 1 % of ϵ change. An increase in emissivity to 0.97 leads to a decrease in Rn, showing a relative sensitivity of -5.0 % per 1 % of ϵ change. A decrease of ϵ to 0.94 generates a relative PS decrease, indicating a sensitivity of -2.4 % per 1 % of ϵ change. The change from 0.958 to 0.97 leads to an increase of PS, denoting a relative sensitivity of 4.6 % per 1 % of ϵ change. The responses of the other fluxes show a relative sensitivity below 1.5 %.

In 2009, the changes of fluxes are similar. Here, the largest relative difference is detected for sensible heat, caused by a decrease in emissivity to $\epsilon = 0.94$, implying a sensitivity of 20.4 % per 1 % of ϵ change. The emissivity increase of 0.012 generates an H decrease, implying a relative sensitivity of -19.3 % per 1 % of ϵ change. In op-

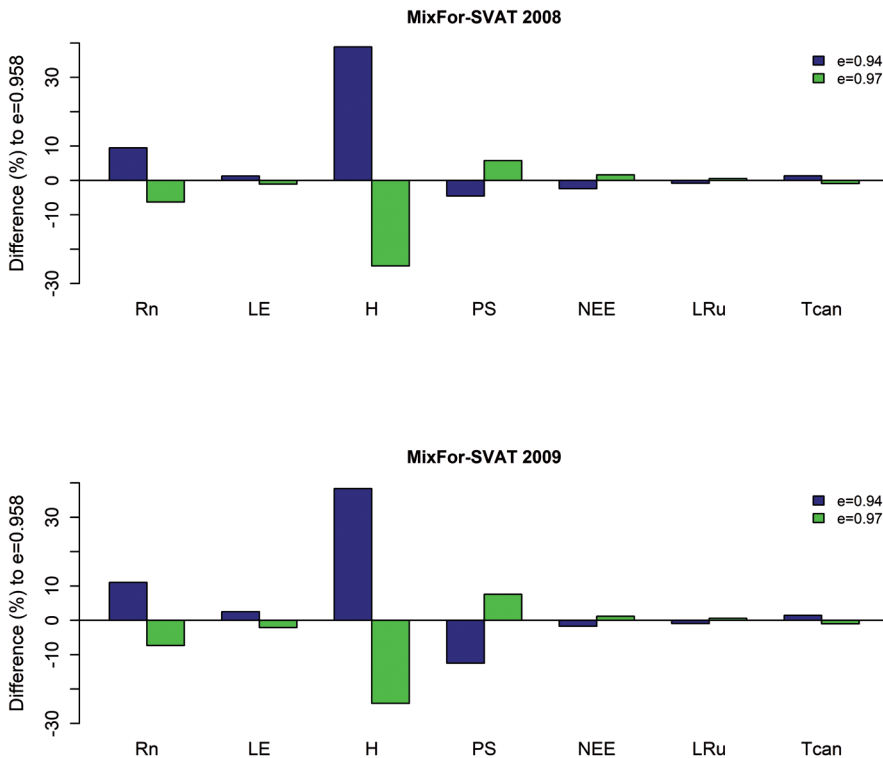


Fig.2. Effects of ϵ changes on the radiative, sensible and latent energy fluxes of Hainich forest. Relative changes of energy fluxes Rn, LE, H, LRU, PS as well as of NEE and Tc to changes in emissivity based on MixFor-SVAT model simulations with emissivities of $\epsilon = 0.94$, $\epsilon = 0.958$ and $\epsilon = 0.97$ for the years 2008 and 2009. The flux values calculated with $\epsilon=0.958$ are taken as the reference. The relative changes are based on mean annual fluxes and calculated according to equation (2)

posite to 2008, Rn and PS show a similar relative change to emissivity changes in 2009. A decrease of ϵ from 0.958 to 0.94 leads to a relative PS decrease, indicating a sensitivity of -6.6 % per 1 % of ϵ change. The change from 0.958 to 0.97 causes an increase of PS, denoting a relative sensitivity of 6.0 % per 1 % of ϵ change. For Rn, a decrease of 0.018 in emissivity produces a relative increase, implying a relative sensitivity of 5.9 % per 1 % of ϵ change. An increase in emissivity to 0.97 leads to an Rn decrease, standing for a sensitivity of -5.8 % per 1 % of ϵ change. All other fluxes show less response to ϵ ; below 2.0 % relative sensitivity. These results indicate that the responses of fluxes to the changes of emissivity are non-linear.

DISCUSSION

So far, only a few studies have been carried out to directly determine broadband emissivities of leaves for forest species resulting in values ranging from 0.94 to 0.97. The leaf emissivities calculated in this study are also within this range (0.958 ± 0.002). No statistically significant differences among species were found except for *Populus simonii* (Table 2). The question is whether this variability has any considerable effect on energy and matter fluxes, and thus, on local and regional climate in forests as was described by Jin and Liang (2006) by means of the coupled atmosphere land surface model CAM2-CLM2 for the emissivity of bare soil (0.9 instead of 0.96). The MixFor-SVAT model applied in this study produced reliable results, well agreeing with the measurements. With increasing ϵ , the value of LRup increases since more longwave radiation is emitted with higher ϵ according to the Stefan-Boltzmann law. When more longwave radiation is lost from the surface, Rn is decreasing as all other fluxes of the radiation budget (incoming shortwave radiation, reflected shortwave radiation and incoming longwave radiation from the atmosphere) are not affected – however, a higher proportion of the incoming longwave radiation will be absorbed ($\epsilon = \alpha$, Kirchhoff's law). At the same time, the surface temperature will decrease leading to a lower sensible heat fluxes as well as low-

er latent heat fluxes. With the decreasing surface temperature, also respiration and photosynthesis are decreasing. As respiration decreases faster than photosynthesis, the net CO₂ uptake is increasing (more negative net ecosystem exchange). The differences in relative changes (Fig. 2) are a consequence of the absolute change and the magnitude of the annual mean fluxes. The annual mean fluxes of H are low due to the negative values at night and wintertime and thus resulting in the largest relative changes. The model, therefore, shows plausible ecosystem responses and can be used for the experiments. The effect of emissivity changes on fluxes found in the present study is considerable, although the absolute values of daily mean changes of fluxes are slightly lower than in Jin and Liang (2006) for desert areas - up to 50 Wm⁻². The differences between $\epsilon = 0.94$ and 0.97 results in changes of daily fluxes up to 16.8 Wm⁻² for Rn, 13.3 Wm⁻² for LE, 19.7 Wm⁻² for H and -10.9 Wm⁻² for LRup. The responses of the system are, thus, quite comparable despite of the different models used for the studies. The lower differences in our study could be explained by the smaller change of ϵ . The changes of daily Tc are, however, comparable with Jin and Liang (2006) - up to 1.1 °C. The response of daily NEE to the ϵ variability is considerable - up to 0.5 $\mu\text{mol C m}^{-2}\text{s}^{-1}$ or 5 kg per day and ha. Moreover, the short time responses at 30 min scales (not shown by Jin and Liang) are even stronger - up to -82.1 Wm⁻² for Rn, 113.8 Wm⁻² for LE and 178.3 Wm⁻² for H. The hourly variability of LRup is of similar order as the daily one, up to -13.9 Wm⁻². The differences in Tc and NEE are also very large: between -2 and 0.5 °C and up to 5.5 $\mu\text{mol C m}^{-2}\text{s}^{-1}$ (2.4 kg C ha⁻¹h⁻¹). Thus, the variability of ϵ should be taken into account in climate change studies. Hence, not only the soil emissivity but also the exact values of leaf emissivities for forest species are crucial information for the better estimation of the contribution of forest ecosystems to climate processes and to climate change. The simple approximation of ϵ is difficult since the dependence of fluxes on ϵ is non-linear, as demonstrated in this study. Moreover, it should be noted that the responses obtained in this study are the di-

rect, “momentarily” ones, as they do not include feedbacks of the climate system to changes in the underlying surface. It is, therefore, recommended to repeat the simulations with a coupled model as in the study of Jin and Liang (2006).

CONCLUSION

In the present study, we quantified the broadband leaf emissivities $\epsilon_{8-14\mu\text{m}}$ of the forest species' *Acer pseudoplatanus*, *Fagus sylvatica*, *Fraxinus excelsior*, *Populus simonii* and *Populus candicans*. The results showed that the interspecies variability of leaf emissivities is very low – the obtained mean value across all species is $\epsilon = 0.958$ (± 0.002). A statistically significant difference was found for *Populus simonii*. Our results demonstrate that emissivity changes have significant impacts on modelled energy and matter fluxes. Energy fluxes and surface temperature increased with a decrease in emissivity, whereas NEE decreased, due to respiration losses resulting from the temperature increase. The strongest effect was identified for the sensible heat flux with a sensitivity of 20.7 % per 1 % of ϵ change. Overall, the findings indicate that the dependency of energy and matter fluxes on ϵ changes are non-linear.

Revealing directly measured leaf emissivities of the five forest species', this study provides important basics for the correct application of variable leaf emissivity in energy budget modelling and thus to a

better estimation of the contribution of forest ecosystems to the climate. Additionally, the application of the obtained emissivity values in MixFor-SVAT showed, that there are strong effects of emissivity changes on radiative, sensible and latent energy fluxes. Therefore, it is recommended to consider the variability of ϵ in climate change studies. Further research should be implemented to extend the knowledge on the forest climate interaction by obtaining information on forest species specific leaf emissivities.

ACKNOWLEDGEMENTS

This study was financially supported by the Deutsche Forschungsgemeinschaft (DFG) (KN 582/6-1) and the Deutsche Bundesstiftung Umwelt (DBU) (20014/352). We are indebted to Andreas Teichmann, Sara Nicke-Mühlfeit, Frank Tiedemann, Dietmar Fellert and Stefan Schütz (University of Göttingen). Measurements at the Hainich tower site were supported by the German Federal Ministry of Education and Research (BMBF) as part of the European Integrated Carbon Observation System (ICOS) and by the Deutsche Forschungsgemeinschaft (INST 186/1118-1 FUGG). ■

REFERENCES

- Alkama R. and Cescatti A. (2016). Biophysical climate impacts of recent changes in global forest cover. *Science*, 351, pp. 600-604. <https://doi.org/10.1126/science.aac8083>.
- Anthoni P.M., Knohl A., Rebmann C., Freibauer A., Mund M., Ziegler W., Kolle O. and Schulze E.D. (2004). Forest and agricultural land-use-dependent CO₂ exchange in Thuringia, Germany. *Global Change Biology*, 10, pp. 2005-2019. doi: 10.1111/j.1365-2486.2004.00863.x.
- Bonan G.B. (2008). Forests and Climate Change: Forcings, Feedbacks, and the Climate Benefits of Forests. *Science*, 320 (5882), pp. 1444-1449. doi: 10.1126/science.1155121.
- Chen C. (2015). Determining the leaf emissivity of three crops by infrared thermometry. *Sensors*, 15(5), pp. 11387-11401. doi:10.3390/s150511387.

Da Luz B.R. and Crowley J.K. (2007). Spectral reflectance and emissivity features of broad leaf plants: Prospects for remote sensing in the thermal infrared (8.0 – 14.0 μm). *Remote Sensing of Environment*, 109(4), pp. 393-405.

Falge E., Reth S., Brüggemann N., Butterbach-Bahl K., Goldberg V., Oltchev A., Schaaf S., Spindler G., Stiller B., Queck R., Köstner B. and Bernhofer C. (2005). Comparison of surface energy exchange models with eddy flux data in forest and grassland ecosystems of Germany. *Ecological Modelling*, 188, pp. 174-216.

Fuchs M. and Tanner C.B. (1966). Infrared thermometry of vegetation. *Agronomy Journal*, 58, pp. 597-601.

Horton K.A., Johnson J.R. and Lucey P.G. (1998). Infrared measurements of pristine and disturbed soils 2. Environmental effects and field data reduction. *Remote Sensing of Environment*, 64(1), pp. 47-52.

Idso S.B., Jackson R.D., Ehler W.L. and Mitchell S.T. (1969). A Method for Determination of Infrared Emittance of Leaves. *Ecology*, 50, pp. 899-902. doi:10.2307/1933705.

Jin, M. and Liang S. (2006). An improved land surface emissivity parameter for land surface models using global remote sensing observations. *Journal of Climate*, 19(12), pp. 2867-2881.

Knohl A., Schulze E.D., Kolle O. and Buchmann N. (2003). Large carbon uptake by an unmanaged 250-year-old deciduous forest in Central Germany. *Agricultural and Forest Meteorology*, 118, pp. 151-167.

Lopez A., Molina-Aiz F.D., Valera D.L. and Peña A. (2012). Determining the emissivity of the leaves of nine horticultural crops by means of infrared thermography. *Scientia Horticulturae*, 137, pp. 49-58.

Oltchev A., Cermak J., Nadezhdina N., Tatarinov F., Tishenko A., Ibrom A. and Gravenhorst G. (2002). Transpiration of a mixed forest stand: field measurements and simulation using SVAT models. *Boreal Environmental Research*, 7(4), pp. 389-397.

Olchev A., Ibrom A., Ross T., Falk U., Rakkibu G., Radler K., Grote S., Kreilein H. and Gravenhorst G. (2008). A modelling approach for simulation of water and carbon dioxide exchange between multi species tropical rain forest and the atmosphere. *Ecological Modelling*, 212, 122-130.

Olchev A., Ibrom A., Panferov O., Gushchina D., Kreilein H., Popov V., Propastin P., June T., Rauf A., Gravenhorst G., Knohl A. (2015). Response of CO_2 and H_2O fluxes in a mountainous tropical rainforest in equatorial Indonesia to El Niño events. *Biogeosciences*, 12, pp. 6655-6667.

Pielke R.A., Pitman A., Niyogi D., Mahmood R., McAlpine C., Hossain F., Goldewijk K.K., Nair U., Betts R., Fall S., Reichstein M., Kabat P., Noblet N. (2011). Land use/land cover changes and climate: modeling analysis and observational evidence. *WIREs Climate Change*, 2, pp. 828-850. doi:10.1002/wcc.144.

Rahkonen J. and Jokela H. (2003). Infrared radiometry for measuring plant leaf temperature during thermal weed control treatment. *Biosystems Engineering*, 86, pp. 257-266.

Sabajo C.R., le Maire G., June T., Meijide A., Roupsard O. and Knohl A. (2017). Expansion of oil palm and other cash crops causes an increase of the land surface temperature in the Jambi province in Indonesia. *Biogeosciences*, 14, pp. 4619-4635. doi.org/10.5194/bg-14-4619-2017.

Snyder P.K., Delire C. and Foley J. (2004). Evaluating the influence of different vegetation biomes on the global climate. *Climate Dynamics*, 23, pp. 279-302.

Valor E. and Caselles V. (1996). Mapping Land Surface Emissivity from NDVI: Application to European, African, and South American Areas. *Remote Sensing of Environment*, 57, pp. 167-184.

Wolfe W.L. and Zissis G.J. (1978). *The Infrared Handbook*. Washington DC, Environmental Research Institute of Michigan.

Zhou L., Dickinson R., Dirmeyer P., Chen, H., Dai D. and Tian Y. (2008). Asymmetric response of maximum and minimum temperatures to soil emissivity change over the Northern African Sahel in a GCM. *Geophysical Research Letters*, 35, L05402. doi:10.1029/2007GL032953.

Received on Dec 31st 2018

Accepted on May 17th 2019

Appendix
Table A.1. Leaf emissivities ($\epsilon \pm$ s.d.) of different plant species

species	ϵ	s.d.	reference
<i>Hedera helix</i> var. <i>Algerian</i>	0.969	0.005	Idso et al. (1969)
<i>Acer pseudoplatanus</i>	0.959	0.003	Tiralla et al. (2019)*
<i>Acer rubrum</i>	0.942 - 0.973		Da Luz & Crowley (2007)
<i>Aralia seboldi</i>	0.968	0.006	Idso et al. (1969)
<i>Brassica rapa</i> L.	0.980	0.010	Rahkonen & Jakela (2003)
<i>Capsicum annuum</i>	0.978	0.008	Lopez et al. (2012)
<i>Capsicum frutescens</i> cv. Long Green	0.979	0.005	Idso et al. (1969)
<i>Carica papaya</i>	0.988	0.002	Idso et al. (1969)
<i>Catalpa speciosa</i>	0.938 - 0.973		Da Luz & Crowley (2007)
<i>Cereus bridges</i> II	0.973	0.001	Idso et al. (1969)
<i>Citrullus lanatus</i> Thunb.	0.981	0.009	Lopez et al. (2012)
<i>Citrus aurantium</i>	0.972	0.008	Idso et al. (1969)
<i>Citrus jambhiri</i>	0.975	0.008	Idso et al. (1969)

<i>Cocculus laurifolius</i>	0.973	0.003	Idso et al. (1969)
<i>Cordyline terminalis</i>	0.967	0.003	Idso et al. (1969)
<i>Cornus florida</i>	0.962 - 0.985		Da Luz & Crowley (2007)
<i>Cucumis melo</i> L.	0.978	0.006	Lopez et al. (2012)
<i>Cucumis sativus</i> L.	0.983	0.008	Lopez et al. (2012)
<i>Cucurbita pepo</i> L.	0.985	0.007	Lopez et al. (2012)
<i>Fagus grandifolia</i>	0.940 - 0.970		Da Luz & Crowley (2007)
<i>Fagus sylvatica</i>	0.960	0.003	Tiralla et al. (2019)*
<i>Fraxinus excelsior</i>	0.958	0.002	Tiralla et al. (2019)*
<i>Gossypium barbadense</i> cv. Pima S-4	0.979	0.008	Idso et al. (1969)
<i>Gossypium hirsutum</i> cv. Deltapine 16	0.964	0.007	Idso et al. (1969)
<i>Gossypium hirsutum</i> cv. Hopicala	0.967	0.011	Idso et al. (1969)
<i>Hedera helix</i> var. Algerian	0.969	0.005	Idso et al. (1969)
<i>Ligustrum vulgare</i> cv. Japanese	0.964	0.003	Idso et al. (1969)
<i>Liriodendron tulipifera</i>	0.948 - 0.973		Da Luz & Crowley (2007)
<i>Lophocereus schottii</i>	0.973	0.004	Idso et al. (1969)
<i>Lycopersicon esculentum</i> cv. Pearson Improved	0.982	0.004	Idso et al. (1969)
<i>Lycopersicon esculentum</i>	0.980	0.010	Lopez et al. (2012)
<i>Morus alba</i>	0.976	0.008	Idso et al. (1969)
<i>Nicotiana tabacum</i>	0.971	0.002	Fuchs & Tanner (1966)
<i>Nicotiana tabacum</i>	0.972	0.006	Idso et al. (1969)
<i>Nymphaea odorata</i>	0.957	0.006	Idso et al. (1969)
<i>Opuntia basilaris</i>	0.978	0.002	Idso et al. (1969)
<i>Opuntia engelmannii</i>	0.961	0.004	Idso et al. (1969)
<i>Opuntia ficus indica</i>	0.957	0.002	Idso et al. (1969)
<i>Opuntia linguiformis</i>	0.965	0.001	Idso et al. (1969)
<i>Opuntia orbiculate</i>	0.710	0.006	Idso et al. (1969)
<i>Opuntia rufida</i>	0.977	0.002	Idso et al. (1969)

<i>Opuntia santa rita</i>	0.969	0.002	Idso et al. (1969)
<i>Pachira macrocarpa</i>	0.985	0.005	Chen (2015)
<i>Paphiopedilum</i> var. Michael Koopowitz	0.981	0.007	Chen (2015)
<i>Pelargonium domesticum</i> var. Martha Washington	0.992	0.002	Idso et al. (1969)
<i>Persea drymifolia</i>	0.979	0.009	Idso et al. (1969)
<i>Phalaenopsis</i> var. Taisuco Anna (mature leaves)	0.981	0.010	Chen (2015)
<i>Phalaenopsis</i> var. Taisuco Anna (young leaves)	0.978	0.009	Chen (2015)
<i>Phaseolus coccineus</i>	0.983	0.005	Lopez et al. (2012)
<i>Phaseolus vulgaris</i> cv. Bountiful (center leaflet)	0.938	0.008	Idso et al. (1969)
<i>Phaseolus vulgaris</i> cv. Bountiful (lateral leaflet)	0.964	0.005	Idso et al. (1969)
<i>Phaseolus vulgaris</i> L.	0.983	0.006	Lopez et al. (2012)
<i>Phaseolus vulgaris</i> L.	0.957	0.005	Fuchs & Tanner (1966)
<i>Philodendron selloum</i>	0.990	0.010	Idso et al. (1969)
<i>Populus candicans</i>	0.957	0.003	Tiralla et al. (2019)*
<i>Populus fremontii</i>	0.977	0.004	Idso et al. (1969)
<i>Populus simonii</i>	0.954	0.003	Tiralla et al. (2019)*
<i>Prunus serotina</i>	0.945 - 0.967		Da Luz & Crowley (2007)
<i>Rosa</i>	0.993	0.006	Idso et al. (1969)
<i>Saccharum officinarum</i>	0.995	0.004	Idso et al. (1969)
<i>Solanum melongena</i> L.	0.973	0.007	Lopez et al. (2012)
<i>Sonchus arvensis</i>	0.980	0.010	Rahkonen & Jakela (2003)
<i>Zea mays</i> cv. Mexican June	0.944	0.004	Idso et al. (1969)

* this study